A Multinuclear NMR Study on the Structure and Dynamics of Lanthanide(III) Complexes of the Poly(amino carboxylate) $EGTA^{4-}$ in Aqueous Solution

Silvio Aime,*,† Alessandro Barge,† Alain Borel,‡ Mauro Botta,† Sergei Chemerisov,§ André E. Merbach,*,‡ Ute Müller,‡ and Dirk Pubanz‡

Dipartimento di Chimica IFM, University of Torino, Via Pietro Giuria 7, I-10125 Torino, Italy, Institute of Inorganic and Analytical Chemistry, University of Lausanne, BCH, CH-1015 Lausanne, Switzerland, and Institute of Chemical Physics, Russian Academy of Science, 117977 Moscow V-334, Kosygina 4, Russia

Received February 27, 1997[⊗]

The structures and intramolecular dynamics of $[Ln(EGTA)(H_2O)]^-$ (Ln = La^{3+}, Ce^{3+}, Pr^{3+}, Nd^{3+}, Sm^{3+}, Eu^{3+}, Gd^{3+}, Tb^{3+}, Dy^{3+}, Ho^{3+}, Er^{3+}, Tm^{3+}, Yb^{3+}, Lu^{3+} and $EGTA^{4-}$ = 3,12-bis(carboxymethyl)-6,9-dioxa-3,12-diazatetradecanedioate(4−)) in aqueous solution have been investigated by variable temperature ^1H and ^{13}C NMR. The quantitative analysis of the proton hyperfine shifts and considerations about the stereochemical nonrigidity indicate the occurrence of a structural change along the lanthanide series with the crossover between Sm and Eu. Changes of coordination number from 10 to 9 to 8 are proposed to occur across the series. The experimental data from ^{17}O NMR, EPR and NMRD studies for the Gd^{3+} complex are treated using a self-consistent theoretical model in a simultaneous multiple parameter least-squares fitting procedure (Powell, D. H.; Ni Dhubhghaill, O. M.; Pubanz, D.; Helm, L.; Lebedev, Y. S.; Schlaepfer, W.; Merbach, A. E. *J. Am. Chem. Soc.* **1996**, *118*, 9333). An intermolecular dipole−dipole electronic relaxation mechanism that has very recently been described for Gd^{3+} complexes (Powell et al., op. cit.) is included in the data treatment. The high water exchange rate of $[Gd(EGTA)(H_2O)]^-$ of $k_{ex}^{298} = (3.1 \pm 0.2) \times 10^7\ s^{-1}$ is explained in terms of a limiting dissociative exchange mechanism ($\Delta V^{\ddagger} = +10.5 \pm 1.0\ cm^3mol^{-1}$), favored by the steric constraints on the water binding site that are revealed by the study on the solution structure.

Introduction

Poly(amino carboxylate) ligands have been widely used as ligands for lanthanide(III) ions. A large variety of structural arrangements has been designed and synthesized in order to meet the exact requirements for specific applications. The ligands may be tailored to fine-tune the kinetic and thermodynamic stabilities of the resulting complexes according to the application in which they are to be used, e.g., as sequestering agents or as diagnostic tools in medicine. Among the latter applications, the use as contrast agents (CA) for magnetic resonance imaging (MRI) has attracted much attention in recent years.

A broad data base has already been acquired concerning the stability constants of lanthanide(III) poly(amino carboxylate) complexes[2] and is still being enlarged.[3,4] The specific application as CA for MRI prompted the search for relationships between structural and dynamic properties of lanthanide(III) poly(amino carboxylate) complexes, including their hydration shell and the relaxation behavior of the center metal's unpaired electrons. The ligands used mostly have a denticity of 8 and are derivatives of either H_5DTPA (1,1,4,7,7-pentakis(carboxymethyl)-1,4,7-triazaheptane) or H_4DOTA (1,4,7,10-tetrakis(carboxymethyl)-1,4,7,10-tetraazacyclododecane), often referred to as the linear and cyclic synthons, respectively. $DTPA^{5-}$ provides a set of three nitrogen and five oxygen donor atoms which usually wrap the metal in a bicapped trigonal prismatic structure,[5] whereas the preformed cavity formed by the four nitrogen and four oxygen atoms of $DOTA^{4-}$ coordinates the lanthanide in a square antiprismatic arrangement.[6] In this paper we show that the integrated NMR study on the structural and dynamic behavior of $[Ln(EGTA)(H_2O)_x]^-$ (see Chart 1 for the structure) complexes in aqueous solution[7] provides further insights to a systematic understanding of the relationship between structure and dynamics in this highly useful class of lanthanide(III) poly(amino carboxylate) complexes.

Experimental Section

Structural Studies. The ligand $EGTA^{4-}$ and the lanthanide(III) oxides were purchased from Aldrich Chemical Co. The complexes were prepared as potassium salts in aqueous solution by mixing stoichiometric amounts of lanthanide(III) oxide, the ligand in the free acid form, and potassium hydroxide. The suspension was heated to

* Author to whom correspondence should be addressed. Tel: +39 11 670 7520. Fax: +39 11 670 7524. E-mail: aime@ch.unito.it.
† University of Torino.
‡ University of Lausanne.
§ Russian Academy of Science.
⊗ Abstract published in *Advance ACS Abstracts*, September 15, 1997.

(1) Powell, D. H.; Ni Dhubhghaill, O. M.; Pubanz, D.; Helm, L.; Lebedev, Y. S.; Schlaepfer, W.; Merbach, A. E. *J. Am. Chem. Soc*. **1996**, *118*, 9333.
(2) Martell, A. E.; Smith, R. M. *Critical Stability Constants*; Plenum Press: New York, 1974; Vol. 1.
(3) Burai, L.; Jakab, S.; Király, R.; Lázár, I.; Tóth, I.; Brücher, E. *J. Chem. Soc., Dalton Trans.* **1996**, 1113.
(4) Sherry, A. D.; Ren, J.; Huskens, J.; Brücher, E.; Tóth, É.; Geraldes, C. F. G. C.; Castro, M. M. C. A.; Cacheris, W. P. *Inorg. Chem.* **1996**, *35*, 4604.
(5) (a) Jenkins, B. G.; Lauffer, R. B. *Inorg. Chem*. **1988**, *27*, 4730. (b) Peters, J. A. *Inorg. Chem.* **1988**, *27*, 4686. (c) Aime, S.; Botta, M. *Inorg. Chim. Acta* **1990**, *177*, 101. (d) Stezowski, J. J.; Hoard, J. L. *Isr. J. Chem.* **1984**, *24*, 323.
(6) (a) Desreux, J. F. *Inorg. Chem.* **1980**, *19*, 1319. (b) Aime, S.; Botta, M.; Ermondi, G. *Inorg. Chem.* **1992**, *31*, 4291. (c) Aime, S.; Barge. A.; Botta, M.; Fasano, M.; Ayala, J. D.; Bombieri, G. *Inorg. Chim. Acta* **1996**, *246*, 423.
(7) (a) Holz, R. C.; Klakamp, S. L.; Chang, C. A.; Horrocks, W. D., Jr. *Inorg. Chem*. **1990**, *29*, 2651. (b) Aime, S.; Botta, M.; Nonnato, A.; Terreno, E.; Anelli, P. L.; Uggeri, F. *J. Alloys. Compd.* **1995**, *225*, 274.

S0020-1669(97)00240-1 CCC: $14.00

Chart 1. The Structure of the Ligand EGTA^{4-} with the Labeling Used To Assign the Resonances and the Positions of the Atoms on the Coordination Polyhedrons

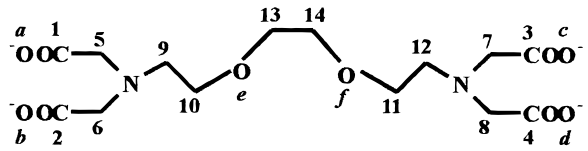

360 K and stirred until a clear solution was obtained; the reaction time depends strongly on the lanthanide. The solution was filtered and the solvent evaporated under reduced pressure to give the complex in the form of its potassium salt as a white solid in 90% yield. The complexes were dissolved in D_2O, and the pD was adjusted to 7.0 by addition of DCl or KOD and checked with a glass electrode connected to an Orion pH-meter. The spectra were recorded at 2.1 T (90 MHz, ^{1}H; 22.6 MHz, ^{13}C) on a JEOL EX-90 and at 9.4 T (400.0 MHz, ^{1}H; 100.6 MHz, ^{13}C) on a JEOL EX-400 spectrometer. The temperature was controlled with JEOL thermostating units and measured by the chemical shift difference of the methanol resonances, calibrated with a thermocouple inside in an NMR tube in the 2.1 T electromagnet. All solutions (0.05−0.1 mol kg^{-1}) contained 1% of Bu^{t}OH as an internal chemical shift reference.

The partial deuteration of the four acetate groups of EGTA^{4-} was obtained by a method similar to that described by Lauffer *et al.*:[5a] a solution of the ligand in D_2O at pD = 10.5 (NaOD) was stirred at 358 K for 45 h. Integration of the ^{1}H resonances indicated a 50% deuteration of the acetate protons. The partially deuterated ligand was used to prepare lanthanide complexes in order to allow the assignment of the acetate signals in the corresponding ^{1}H NMR spectra.

Relaxation Measurements. Sample Preparation. All solutions were prepared gravimetrically. The solid gadolinium complex obtained as described above was dissolved in doubly distilled water and the pH, measured with a combined glass electrode calibrated with Metrohm buffers, was adjusted by adding weighted amounts of aqueous solutions of perchloric acid or sodium hydroxide of known concentration. The absence of free metal was checked by the xylenol orange test.[8] ^{17}O-Enriched water (11%, Yeda R&D Co., Rehovot, Israel) was added to the solutions for the ^{17}O NMR measurements (final enrichment ca. 2%) to increase sensitivity, and the pH was checked again.

EPR. The EPR spectra were measured at the X-band (Lausanne) and the 2-mm band (Moscow). All spectrometers were operated in the continuous wave mode. The 2-mm spectrometer in Moscow is home built; the X-band spectrometer was manufactured by Bruker. All measurements at the 2-mm band were performed with a semifocal Fabri-Perot resonator. For the 2-mm-band measurements, the samples were contained between two quartz plates;[9] for X-band, the samples were in 1-mm quartz tubes. The acquisition parameters, especially modulation amplitude and microwave power, were varied and the final spectra recorded with values that did not affect the line width. The peak-to-peak line width was measured from the recorded spectrum either with a ruler or using instrument software. The cavity temperature was stabilized using electronic temperature control of gas flowing through the cavity. For the X-band measurements, the temperature was verified by substituting a thermometer for the sample tube. At the 2-mm band, the temperature was measured using a thermocouple built into the probehead. Measurements were made at temperatures from 273.2 K to the maximum obtainable for each instrument.

^{17}O NMR. Variable temperature ^{17}O NMR measurements were performed at three different magnetic fields using Bruker AMX2-600 (14.1 T, 81.2 MHz), AM-400 (9.4 T, 54.2 MHz), and AC-200 (4.7 T, 27.1 MHz) spectrometers and a WP-60 electromagnet (1.4 T, 8.1 MHz) adapted for use with the AC-200 console. Bruker VT-1000 temperature control units were used to stabilize the temperature, which was measured by a substitution technique.[10] The samples were sealed in glass spheres, fitting into 10 mm NMR tubes, in order to eliminate susceptibility

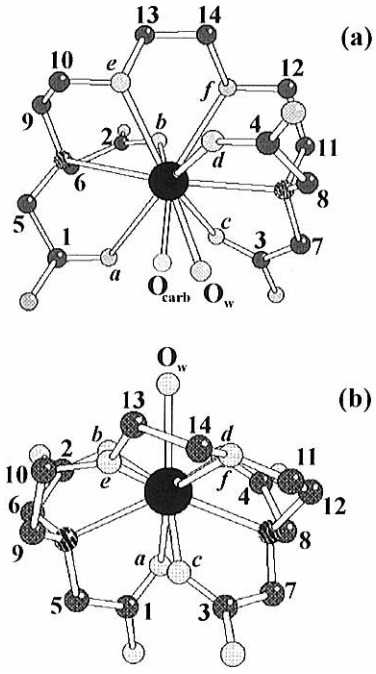

Figure 1. The crystal structure of [Nd(EGTA)(H$_2$O)]$^-$ (a) and of [Er(EGTA)(H$_2$O)]$^-$ (b).

corrections to the chemical shift.[11] Longitudinal relaxation rates, $1/T_1$, were obtained by the inversion recovery method,[12] and transverse relaxation rates, $1/T_2$, by the Carr−Purcell−Meiboom−Gill spin echo technique,[13] or (for line widths greater than 1 kHz) directly from the line widths.

NMRD Measurements. The longitudinal proton relaxivity of K[Gd(EGTA)(H$_2$O)] in aqueous solution as a function of the magnetic field strength from 2.5×10^{-4} to 1.4 T (0.01−60 MHz) was measured on the Koenig−Brown field cycling relaxometer[14] at the University of Florence, Italy. The temperature was controlled by circulating Freon from an external bath and measured by a thermometer inserted into the Freon close to the sample.

The variable temperature and pH dependence of the longitudinal relaxation of water protons at 20 MHz was investigated on a Stelar Spinmaster spectrometer from Stelar, Mede (PV), Italy. The standard inversion−recovery technique was used with a typical 90° pulse width of 3.5 μs, 16 experiments with 4 scans. The temperature was controlled by a Stelar VTC-91 airflow heater, equipped with a copper−constantan thermocouple. The actual temperature of the sample was measured with a Fluke 52 K/j digital thermometer with an uncertainty of ±0.5 K.

Structural drawings were produced by using Moldraw.[15]

Results

Solution Structure. In the solid state [Nd(EGTA)(H$_2$O)]$^-$ displays a 10-fold coordination.[16] It is achieved by coordination of the octadentate ligand, an inner sphere water molecule, and a carboxylate oxygen belonging to an adjacent molecule. The coordination polyhedron (Figure 1a) can be described as a distorted bicapped square antiprism where the capping positions are occupied by the two nitrogen atoms. The square faces,

(8) Brunisholz, G.; Randin, M. *Helv. Chim. Acta* **1959**, *68*, 508.
(9) Lebedev, Y. S. In *Modern Pulsed and Continuous Wave Electron Spin Resonance*; Kevan, L., Bowman, M., Eds.; Wiley: New York, 1990.
(10) Ammann, C.; Meier, P.; Merbach, A. E. *J. Magn. Reson.* **1982**, *46*, 319.
(11) Hugi, A. D.; Helm, L.; Merbach, A. E. *Helv. Chim. Acta.* **1985**, *68*, 508.
(12) Vold, R. V.; Waugh, J. S.; Klein, M. P.; Phelps, D. E. *J. Chem. Phys.* **1968**, *48*, 3831.
(13) Meiboom, S.; Gill, D. *Rev. Sci. Instrum.* **1958**, *29*, 688.
(14) Koenig, S. H.; Brown, R. D., III. *NMR Spectroscopy of Cells and Organisms*; Gupta, R. K., Ed.; CRC Press: Boca Raton, FL, 1987; Vol. II.
(15) Ugliengo, P.; Borzani, G.; Viterbo, D. *J. Appl. Crystallogr.* **1988**, *21*, 75.
(16) Schauer, C. K.; Anderson, O. P. *J. Chem. Soc., Dalton Trans.* **1989**, 185.

Scheme 1

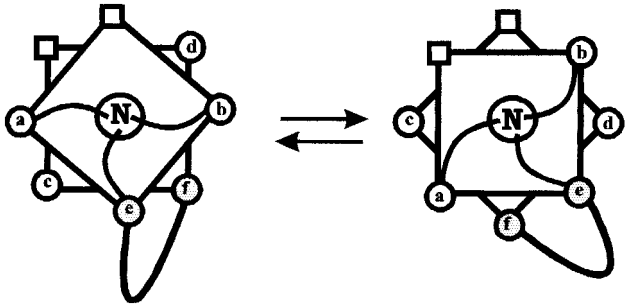

linked by the diether bridge, are each formed by one of the ether oxygens, two oxygen atoms of adjacent carboxylate groups, and respectively, the water molecule or a carboxylate oxygen of an adjacent molecule. In solution one expects the complex either to maintain its 10-fold coordination by binding a second water molecule into the inner sphere forming $[Nd(EGTA)(H_2O)_2]^-$ (see Scheme 1) or to reduce its coordination number to 9. In this latter case, the change in the coordination number is probably accompanied by a rearrangement of the coordination polyhedron in order to minimize the steric strain. UV−vis spectra for the Eu^{3+} complex show a single band at 580 nm in solution as a function of temperature for the $^7F_0 \rightarrow {}^5D_0$ transition. This is indicative of the presence of a single species assigned as the ennea-coordinated complex $[Eu(EGTA)(H_2O)]^-$ by analogy with the ^{17}O NMR based assignment made for the Gd^{3+} complex (see below). UV−vis spectra from 220 to 350 nm of the Ce^{3+} complex at variable temperature and pressure prove the presence of two species, which are assigned to an equilibrium ($K_{10\rightarrow 9}{}^{298} = 0.7 \pm 0.1$, $\Delta V_{10\rightarrow 9}{}^0 = +15.9 \pm 1.5$ cm^3 mol^{-1}, see supporting information) between a deca- and an ennea-coordinated complex on the basis of the larger ionic radius of Ce^{3+}. In analogy with the solid state structure the deca-coordinated complexes should display an effective C_2 symmetry. The symmetry axis passes through the C−C bond of the diether bridge and the middle of the edge between two oxygen atoms belonging to carboxylate groups at opposite ends of the ligand. The C_2 symmetry axis creates pairs of chemically equivalent protons and carbon nuclei, and thus 10 proton and seven carbon resonances are expected in the NMR spectra in the absence of fluxional processes. Analogous spectral patterns would also be expected in the case of fast (on the NMR time scale) isomerization between the deca- and ennea-coordinated species.

At room temperature only five resonances are present in both the proton and the carbon NMR spectra of the diamagnetic La^{3+} chelate (see Figure 2). The proton spectrum shows one singlet for the four ethylenic protons of the diether bridge ($\delta = 3.87$ ppm), two singlets for the methylene protons of the ether−nitrilo ethylene groups ($\delta = 2.88$ and 3.81 ppm), and one AB spin system for the eight acetate protons (3.34 and 3.63 ppm; $^2J = 16.7$ Hz). Accordingly, the four carbonyl carbons generate one signal, and likewise do the four methylenic carbons of the acetate arms. Thus, a fast rearrangement averages the signals of pairs of atoms at room temperature. The most likely conformational change able to cause such averaging is a rotation of the two ligand halves around the C−C bond of the diether bridge, which scrambles the position of the acetate groups. The schematic representation (Scheme 1) shows the process as a 45° rotation of the two square faces in opposite directions. At 273 K an incipient broadening of all resonances indicates that a dynamic process is slowing down and provides support to our interpretation.

Basically the same features are found in the spectra of the $EGTA^{4-}$ complexes of the lighter paramagnetic lanthanides up to Sm^{3+} (see Figure 3). Their proton spectra show five resonances (and five also in the carbon spectra) that broaden considerably on lowering the temperature. The further one proceeds down along the series, and the higher is the temperature at which the exchange broadening starts. This indicates that as the metal ion gets smaller, the complex gains in stereochemical rigidity. This indication is only qualitative since no attempts were made to obtain kinetic parameters, but it is plausible if

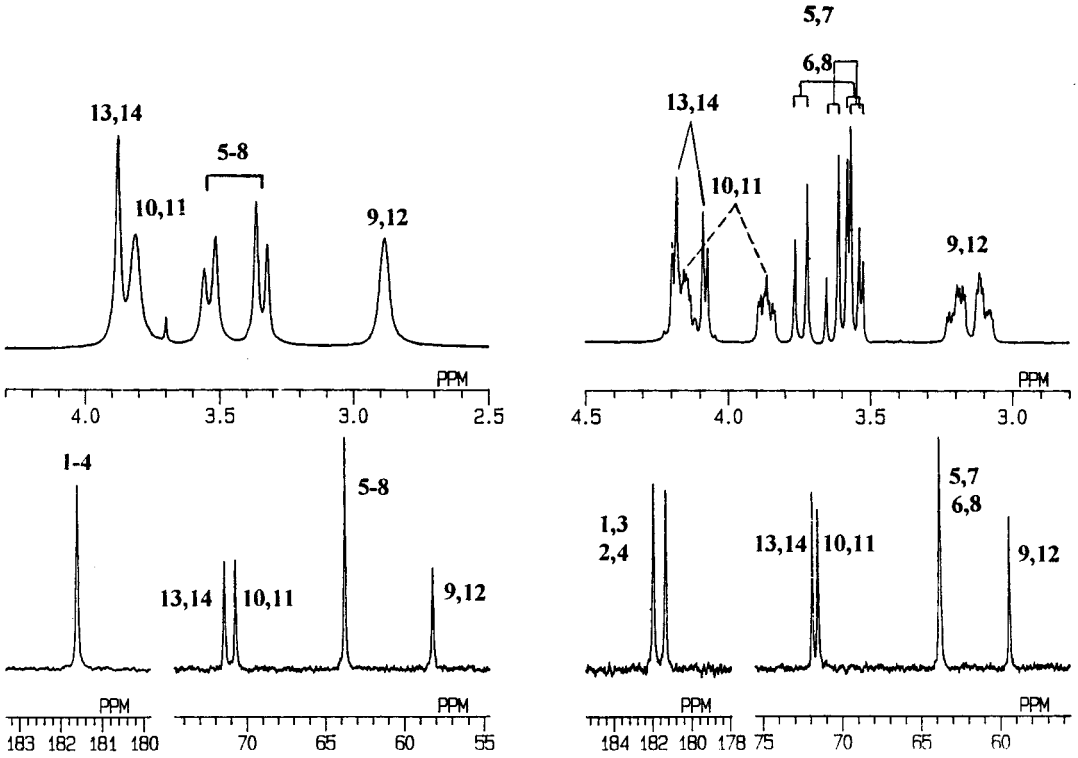

Figure 2. ^1H (top) and ^{13}C (bottom) NMR spectra of the La^{3+} (left) and Lu^{3+} (right) complexes of $EGTA^{4-}$ at 9.4 T and 298 K.

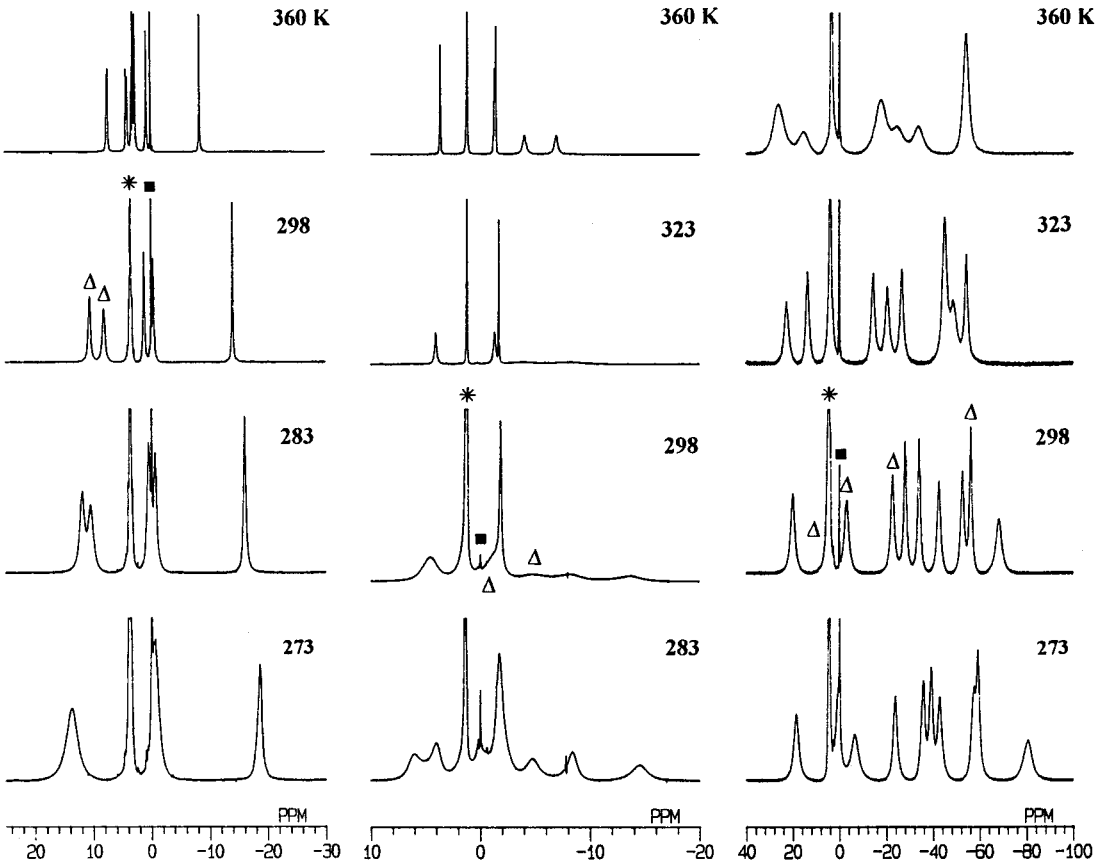

Figure 3. Variable temperature ^{1}H NMR spectra of the Pr^{3+} (left), Eu^{3+} (middle), and Ho^{3+} (right) complexes of $EGTA^{4-}$ at 2.1 T. The resonances labeled with *, ■, and △ refer to solvent, Bu^{t}OH, and acetate protons, respectively.

we consider that the chemical shift difference between the two proton resonances at high frequency (acetate protons; see below) involved in the dynamic process is basically the same from Ce− to Sm−EGTA. Partly due to its relatively greater chemical shift range, but mainly caused by its increased rigidity, the Eu^{3+} complex shows 10 signals in the proton spectrum at 283 K already, as expected for a rigid structure.

The ^{13}C spectrum of $[Eu(EGTA)(H_2O)]^-$ at 273 K shows seven resonances. Coalescence of the carbonyl signals is reached at 300 K. The Eu^{3+} complex is the lightest lanthanide complex of $EGTA^{4-}$ for which the exchange can be rendered slow in the ^{13}C NMR spectrum. From the coalescence temperatures in the ^{13}C spectra a free activation energy of 50 kJ mol^{-1} can be estimated, which is comparable to the values found for similar rearrangements of the corresponding $DTPA^{5-}$ and $DOTA^{4-}$ complexes.[5a,6]

The spectra of the heavier lanthanide(III) complexes of $EGTA^{4-}$ reproduce the features found in the spectrum of the Eu^{3+} complex: at room temperature there are invariably 10 proton and seven carbon resonances, which progressively sharpen up as one moves toward the end of the lanthanide series. This could be interpreted as the continuation of the trend found for the lighter lanthanides: increasing rigidity due to the reduced ionic radius of the center metal. However, the variable temperature spectra in Figure 3 suggest that a second exchange process occurs at lower temperatures with respect to the one described for the complexes of the lighter lanthanides: while the broadening of resonances due to the first rearrangement appears always at higher temperatures, another broadening becomes visible at lower temperature. For example, the proton spectrum of Ho^{3+} (see Figure 3) shows 10 resonances at 298 K, which are broadened at higher *and* lower temperatures. This behavior suggests that a different solution structure has to be assigned to the complexes with the lanthanides heavier than Eu^{3+}, possibly characterized by the magnetic inequivalence of all of the ligand atoms, but undergoing an interconversion that above 273 K is fast on the proton NMR time scale to result in spectra characterized by 10 (exchange broadened) proton resonances and seven carbon resonances.

This view is supported by the solid state structure of the Er^{3+} complex (Figure 1b):[16] the metal ion is 9-coordinate (Nd^{3+} is 10-coordinate), with one inner sphere water oxygen and a coordination polyhedron that is described as a tricapped trigonal prism rather than a capped square antiprism (the latter being the proper description for the coordination polyhedron around Nd^{3+} as discussed above). The capping positions are occupied by the two nitrogen atoms and the inner sphere water oxygen, and the trigonal faces are formed by the oxygen atoms of the ether and the carboxylate groups. According to this description, all 20 protons and 14 carbons are magnetically inequivalent and should therefore generate separate resonances in their NMR spectra. Collapsing these to 10 proton and seven carbon resonances can successfully be explained by the rapid scrambling of two carboxylate groups situated on adjacent vertices of the two trigonal planes, connected by the edge opposite to the capping position of the inner sphere water molecule (Scheme 2).

Structure Assessment from Hyperfine Shifts. Up to this point the suggestion for a structural change along the Ln(III) series leans on the observed temperature behavior of the NMR properties and on the available solid state structures. A thorough proof of a changeover in structure in solution has been gained by the analysis of the lanthanide-induced shifts (LIS) as follows. Observed (obsd) LIS values are a sum of scalar (sc), dipolar (dip), and diamagnetic (dia) contributions, as depicted in eq

Scheme 2

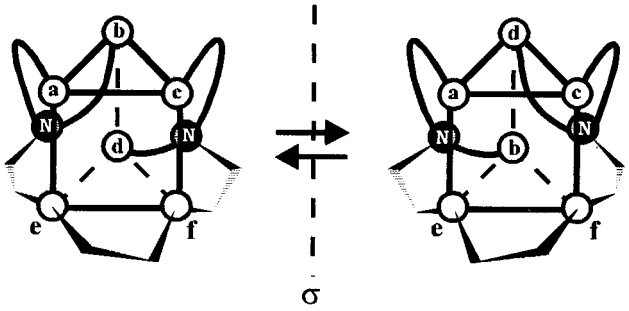

1.[17−19] The geometric information is contained in the dipolar

$$\delta^{obsd} = \delta^{sc} + \delta^{dip} + \delta^{dia} \quad (1)$$

contribution, which can be separated from the other contributions by first subtracting the diamagnetic shift measured on the corresponding diamagnetic Ln^{3+} complexes. The remaining hyperfine shift δ_p can then be separated according to the structure independent method by Reilley *et al.*[17] in eq 2, where

$$\delta_p = F_n\langle S_Z\rangle_m + G_n C_m^{\ D} \quad (2)$$

F_n depends on the observed nucleus and is independent of the lanthanide, $\langle S_Z\rangle_m$ describes the influence of the lanthanide on the scalar shifts and is found in the literature,[20] G_n contains the geometric information inherent in the dipolar shifts, and $C_m^{\ D}$ is a lanthanide dependent number whose values can be found in the literature.[21] Equation 2 can be rearranged into the linear forms given by eqs 3 and 4. Equation 4 is particularly suited

$$\frac{\delta_p}{C_m^{\ D}} = \frac{F_n\langle S_Z\rangle_m}{C_m^{\ D}} + G_n \quad (3)$$

$$\frac{\delta_p}{\langle S_Z\rangle_m} = \frac{G_n C_m^{\ D}}{\langle S_Z\rangle_m} + F_n \quad (4)$$

for the lanthanide complexes where the dipolar contribution is prevalent ($G_n/F_n \gg 1$). It predicts a linear plot of $\delta_p/\langle S_Z\rangle_m$ against $G_nC_m^{\ D}/\langle S_Z\rangle_m$ for equivalent nuclei in corresponding complexes across the entire lanthanide series under the condition that the complexes are isostructural. The acetate protons of the Ln−EGTA complexes have been chosen for this test. Selective deuteration of these protons can be achieved by refluxing the ligand in D_2O at basic pH for several hours. This allows a straightforward assignment of the corresponding resonances in the proton NMR spectra. At 298 K there are two acetate resonances for the complexes from La to Eu, whereas four are observed for the heavier lanthanides. If the complexes are isostructural, then this difference is only due to a different dynamic behavior: fast exchange for the complexes with the lighter ions and slow exchange for the complexes with the heavier ions. On the contrary, if a structural change occurs along the series, then a break should be observed in the linear plot predicted by eq 4. According to the sign of the $C_m^{\ D}$ values,

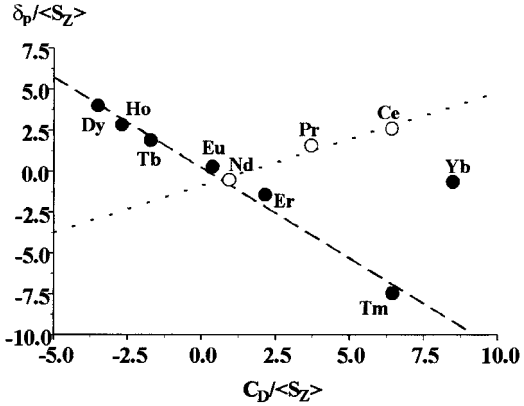

Figure 4. Plots of the Ac1 LIS data for Ln−EGTA (average value of Ac1 and Ac1′ for Ln = Tb−Yb) at 300 K according to eq 4.

we have considered in the analysis the high-frequency acetate peak (Ac1 ≡ Ac1′) for Ce−, Pr−, Nd−, and Eu−EGTA or the average of the two high-frequency (Er, Tm, Yb) or low-frequency (Tb, Dy, Ho) resonances (Ac1 and Ac1′) for the complexes with the heavier lanthanides, in order to mimic fast exchange. The results are shown in Figure 4 and are in agreement with the structural change across the series discussed above: there is a change in the sign of slope from the lighter to the heavier lanthanides with the crossover at Sm^{3+} or Eu^{3+}. Whereas the Eu^{3+} complex itself could perhaps be assigned to both models, it is clear that the structure of the Gd^{3+} complex belongs to the heavier lanthanides. The observed behavior is consistent with the different coordination numbers observed in the two reported crystal structures for Ln−EGTA complexes.[16] The steric crowding of the first coordination sphere causes the loss of one inner sphere water molecule from Sm to Gd, and this loss is accompanied by a conformational change to a tighter, more rigid coordination about the smaller metal ion.

The hyperfine shift of the acetate protons of the Yb^{3+} complex lay outside each of the lines. Additionally, the complexes of Yb^{3+} and Lu^{3+} show a temperature behavior other than that of the complexes of the preceding lanthanides: no exchange broadening at all can be observed for the former. Possibly from Tm to Yb another structural change is taking place. The comparison of the proton spectra in Figure 2 belonging to the La^{3+} and Lu^{3+} complexes, respectively, illustrates the great difference in rigidity that is caused by the variation in radius from one extreme of the lanthanide series to the other. It was proved above that this change in rigidity is caused by a change in conformation that the ligand is undergoing to suit the smaller size of the central ion. The lighter lanthanides (La to Sm) display an equilibrium between deca- and ennea-coordinated forms as shown by UV measurements, yet maintaining the same coordination polyhedron with the water oxygens opposite the ether oxygens (see Figure 1a). The lanthanides from Eu to Tm belong to another structural model (Figure 1b), forming ennea-coordinated complexes with the water oxygen neighboring the ether oxygens. Support for this view comes from the hydration number $q = 1$ measured for Eu−EGTA by Horrocks[7a] and from the fact that we observed a single absorption band for the $^7F_0 \rightarrow {}^5D_0$ transition.[22] The last two members of the series seem to adopt still another solution structure which could be related to the increased availability of an octa-coordinated state without inner sphere water.

Relaxation Properties of the Gd^{3+} Complex. Proton Relaxivity at Constant Field and Variable Temperature. The

(17) Reilley, C. N.; Good, B. W.; Desreux, J. F. *Anal. Chem.* **1975**, *47*, 2110.
(18) Sherry, A. D.; Geraldes, C. F. G. C. In *Lanthanide Probes in Life, Chemical and Earth Sciences: Theory and Practice*; Bünzli, J.-C. G., Choppin, G. R., Eds.; Elsevier: Amsterdam, 1989.
(19) Peters, J. A.; Huskens, J.; Raber, D. J. *Prog. Nucl. Magn. Reson. Spectrosc.* **1996**, *28*, 283.
(20) Golding, R. M.; Halton, M. P. *Aust. J. Chem.* **1972**, *25*, 2577.
(21) Bleaney, B. *J. Magn. Reson.* **1972**, *8*, 91.
(22) Graeppi, N.; Powell, D. H.; Laurenczy, G.; Zékány, L.; Merbach, A. E. *Inorg. Chim. Acta*, **1995**, *235*, 311.

proton relaxivity at 20 MHz has been measured between 273 and 343 K to get a first idea of the potential of Gd−EGTA as an MRI contrast agent. The relaxivity increases by decreasing temperature over the entire range. However, there is a markedly higher relaxivity for the EGTA^{4-} then for the DTPA^{5-} complex below 293 K. The molecular size of the two complexes being very similar, the rotational correlation time cannot be the origin of this difference. The electronic relaxation times of similar complexes are not strongly dependent on temperature,[23] so the only temperature dependent parameter that may account for the difference is the water exchange rate k_{ex}. An integral approach to all relaxation data (EPR, ^{17}O NMR, NMRD), following a procedure recently described,[1] was undertaken on Gd−EGTA (Table 1) in order to assess a potential causal connection between the structure of the complexes and their dynamic parameters, especially their water exchange rate.

Proton Relaxivity at Constant Field and Variable pH. The proton relaxivity of [Gd(EGTA)(H$_2$O)]$^-$ is constant from pH = 3 to pH = 13. This means that in this pH range the complex does not change its number of inner sphere water molecules nor is the inner sphere water molecule protonated or deprotonated. One can safely conclude that in this pH range all eight donor atoms are coordinated to the metal, *i.e.*, the structure of the complex is stable over a change of 10 orders magnitude of proton concentration.

A complete discussion of the theory used below (with all the equations) as well as the description of the fitting of EPR, ^{17}O NMR, and NMRD data can be found in a recent publication.[1] A detailed exposition of the simultaneous multiple parameter fitting is provided as Supporting Information. Here we only give some information which is indispensable for understanding the discussion of the results.

EPR Measurements. In all of the EPR spectra of the Gd^{3+} complex, the line shape was approximately Lorentzian, so the transverse electronic relaxation rates, $1/T_{2e}$, were calculated from the peak-to-peak EPR line widths. The concentration dependent contribution to the line width was treated as relaxation due to intermolecular dipole−dipole interaction by using the parameters[1] obtained for [Gd(DTPA)(H$_2$O)]$^{2-}$. The transverse electronic relaxation rates are shown in the upper box of Figure 5. Electronic relaxation rates in Gd^{3+} complexes have generally been interpreted in terms of a zero field splitting interaction with a small contribution of spin rotation.[23−25] The most important parameters affecting the fit to the EPR data (Table 2) are the mean square of the zero field splitting energy (Δ^2), the correlation time for the modulation of ZFS (τ_v^{298}), and its activation energy (E_v).

Variable Temperature ^{17}O NMR Measurements. From the measured ^{17}O NMR relaxation rates and angular frequencies of the Gd^{3+}-containing solutions and of the acidified water reference one can calculate the reduced relaxation rates and chemical shift, $1/T_{1r}$, $1/T_{2r}$ and $\Delta\omega_r$,[26,27] presented in Figure 5, the second and third boxes from the top.

The ^{17}O longitudinal relaxation rates in Gd^{3+} solutions are governed by the dipole−dipole and quadrupolar mechanisms, and they are essentially in the fast exchange regime (little influence of water exchange). They are thus influenced by four parameters: rotational correlation time (τ_R^{298}), its activation energy (E_R), the Gd−O distance (r_{GdO}), and the quadrupolar coupling constant ($\chi(1+\eta^2/3)^{1/2}$). The ^{17}O transverse relaxation rates in bound water are dominated by the scalar relaxation mechanism.[28] The temperature dependence of the binding time (or inverse exchange rate, $\tau_m = 1/k_{ex}$) of water molecules in the inner sphere allows for determining the activation entropy ($\Delta S^{\ddagger}$), enthalpy ($\Delta H^{\ddagger}$), and the exchange rate at 298.15 K (k_{ex}^{298}).

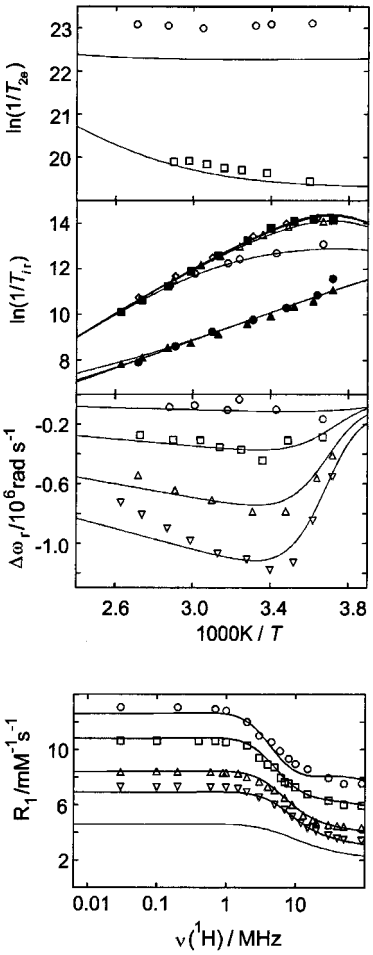

Figure 5. Transverse electronic relaxation rates of [Gd(EGTA)(H$_2$O)]$^-$ at the X-band (0.34 T, ○) and the 2-mm band (5.0 T, □), reduced transverse ^{17}O relaxation rates (■, ◇, △, ○) and chemical shifts (▽, △, □, ○) at 14.1, 9.4, 4.7, and 1.4 T, reduced ^{17}O longitudinal relaxation rates (△, ●) at 14.1 and 9.4 T, and NMRD profiles at 278.2 (○), 286.2 (□), 298.2 (△), and 307.2 K (▽) of aqueous solutions containing [Gd(EGTA)(H$_2$O)]$^-$. The lines represent simultaneous least squares fits to all data points displayed as described in the text with the exception of the lowest line in the bottom box, which shows the outer sphere contribution to proton relaxivity calculated from the fitted parameters at 298.2 K.

Table 1. Compositions of the Different [Gd(EGTA)(H$_2$O)]$^-$ Solutions used in This Study

method	c/mol kg^{-1}	pH
EPR	0.1232	6.0
EPR	0.0126	5.5
EPR	0.1120	4.9
EPR	0.0131	5.0
NMR (VT)	0.097	5.9
NMR (VP)	0.076	6.3
NMRD	0.0015	6.6

NMRD. The proton relaxivities, normalized to millimolar Gd^{3+} concentration, are shown as the bottom box in Figure 5.

(23) Powell, D. H.; Merbach, A. E.; González, G.; Brücher, E.; Micskei, K.; Ottaviani, M. F.; Köhler, K.; von Zelewsky, A.; Grinberg, O. Y.; Lebedev, Ya. S. *Helv. Chim. Acta* **1993**, *76*, 2129.
(24) McLachlan, A. D. *Proc. R. Soc., London* **1964**, *A280*, 271.
(25) Gonzalez, G.; Powell, D. H.; Tissières, V.; Merbach A. E. *J. Phys. Chem.* **1994**, *98*, 53.
(26) Swift, T. J.; Connick, R. E. *J. Chem. Phys.* **1962**, 37, 307.
(27) Zimmermann, J. R.; Brittin, W. E. *J. Phys. Chem.* **1957**, *61*, 1328.
(28) Micskei, K.; Helm, L.; Brücher, E.; Merbach, A. E. *Inorg. Chem.* **1993**, *32*, 3844.

Table 2. Parameters Obtained from the Simultaneous Fitting of EPR, ^{17}O NMR, and NMRD data for Gd^{3+} Complexes[a]

ligand/parameter	aqua[b]	PDTA^{4-}[c]	EGTA^{4-}	DTPA^{5-}[b]	DTPA-BMA^{3-}[b]	DOTA^{4-}[b]
$k_{ex}^{298}/10^6$ s^{-1}	804 ± 60	102 ± 10	31 ± 2	3.3 ± 0.2	0.45 ± 0.01	4.1 ± 0.2
$\Delta H^{\ddagger}$/kJ mol^{-1}	15.3 ± 1.3	11.0 ± 1.4	42.7 ± 3.1	51.6 ± 1.4	47.6 ± 1.1	49.8 ± 1.5
$\Delta S^{\ddagger}$/J mol^{-1} K^{-1}	−23.1 ± 4.0	−54.6 ± 4.6	+42 ± 3	+53.0 ± 4.7	+22.9 ± 3.6	+48.5 ± 4.9
$\Delta V^{\ddagger}$/cm^3 mol^{-1} [d]	−3.3 ± 0.2	−1.5 ± 0.1	+10.5 ± 1.0	+12.5 ± 0.2	+7.3 ± 0.2	+10.5 ± 0.2
$A/\hbar$ /10^6 rad s^{-1}	−5.3 ± 0.1	−4.9 ± 0.2	−3.2 ± 0.1	−3.8 ± 0.2	−3.8 ± 0.2	−3.7 ± 0.2
C_{os}	0.0	0.0	0.1	0.18 ± 0.04	0.11 ± 0.04	0.21 ± 0.04
τ_R^{298}/ps	41 ± 2	79 ± 3	58 ± 6	58 ± 11	66 ± 11	77 ± 4
E_R/kJ mol^{-1}	15.0 ± 1.3	19.2±1.1	25.4 ± 0.6	17.3 ± 0.8	21.9 ± 0.5	16.1 ± 7.4
τ_v^{298}/ps	7.3 ± 0.5	16 ± 2	24 ± 1	25 ± 1	25 ± 1	11 ± 1
E_v/kJ mol^{-1}	18.4 ± 1.4	10.4 ± 2.0	1.0	1.6 ± 1.8	3.9 ± 1.4	1.0
$\Delta^2/10^{20}$ s^{-2}	1.19 ± 0.09	0.80 ± 0.04	0.34 ± 0.02	0.46 ± 0.02	0.41 ± 0.02	0.16 ± 0.01
$\delta g_L^2/10^{-2}$	0.0		2.1 ± 0.3	1.2 ± 0.3	0.8 ± 0.2	1.9 ± 0.3
$D_{GdH}^{298}/10^{-10}$ m^2 s^{-1}	23		20 ± 2	20 ± 3	23 ± 2	22 ± 1
E_{DGdH}/kJ mol^{-1}	22.0		23.2 ± 1.1	19.4 ± 1.8	12.9 ± 2.1	20.2 ± 1.1
$\chi(1+\eta^2/3)^{1/2}$/MHz	7.58/2.0 ± 2.3	7.58	7.58/16 ± 3	7.58/14 ± 2	7.58/18 ± 2	7.58/10 ± 1
r_{GdO}/Å	2.76 ± 0.06/2.5	2.5	2.13 ± 0.04/2.5	2.20 ± 0.09/2.5	2.12 ± 0.04/2.5	2.38 ± 0.03/2.5

[a] Underscored parameters were fixed in the least-squares procedure. [b] See ref 1. [c] From ref 37, parameters calculated without NMRD data. [d] Calculated from ^{17}O data only.

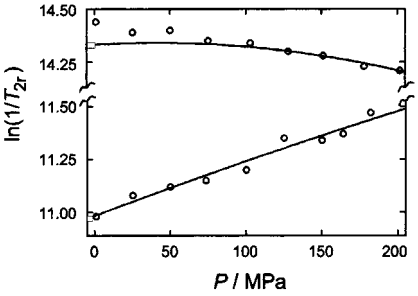

Figure 6. Pressure dependence of the reduced transverse ^{17}O relaxation rates at 9.4 T and 272 K (upper line) and 360 K (lower line) for an aqueous solution of $[Gd(EGTA)(H_2O)]^-$. The lines represent least squares fits as explained in the text.

These NMRD profiles contain contributions from both inner sphere and outer sphere relaxivity.[29] The inner sphere contribution is determined by the number of inner sphere water molecules, the water exchange rate, the rotational correlation time, and the electronic relaxation rates.[30,31] We assume that for both proton and ^{17}O NMR as well as for the spin rotational mechanism τ_R is given by the overall rotational correlation time of the gadolinium−water vector. The outer sphere contribution to proton relaxivity can be described by fitting the diffusion coefficient for diffusion of a water proton away from a Gd^{3+}-complex (D_{GdH}) and its activation energy (E_{DGdH}).[32]

Variable Pressure ^{17}O NMR. The pressure dependence of the reduced transverse relaxation rates, $1/T_{2r}$, for $[Gd(EGTA)(H_2O)]$ at 272.0 and 359.8 K and 9.4 T is shown in Figure 6. At the higher temperature and this magnetic field, $1/T_{2r}$ is in the fast exchange limit and dominated by the scalar interaction. The increase of $1/T_{2r}$ with pressure in Figure 6 (lower line) is, therefore, due to a slowing of the water exchange. At the lower temperature, $1/T_{2r}$ is near the slow exchange limit and so is dominated by τ_m (at higher pressures at least). The decrease of $1/T_{2r}$ with pressure in Figure 6 (upper line) is, therefore, due to a slowing of the water exchange process. The changeover region stretches from zero pressure to about 100 MPa, above which the system is in the slow exchange regime. At low pressure, the fitted line deviates from the experimental points, which seem to stay in the slow exchange regime down to zero pressure. We performed a least squares fit of the data in Figure 6 with $(k_{ex})_0^T$ and $\Delta V^{\ddagger}$ as fitted parameters. The fitted function is shown in Figure 6; the fitted parameters are $(k_{ex})_0^{272} = (8.0 \pm 0.8) \times 10^6$ s^{-1}, $(k_{ex})_0^{360} = (6.7 \pm 0.2) \times 10^8$ s^{-1}, and $\Delta V^{\ddagger} = (+10.5 \pm 1.0)$ cm^3 mol^{-1}.

Discussion

Structure and Rearrangement from Variable Temperature ^1H and ^{13}C NMR. The different solution structures proposed for the lighter and heavier lanthanides can successfully explain all of the NMR data and are compatible with the published solid state structures.

In earlier publications[33] we stated that steric constraints on the water binding site determine the mechanism and the rate of the water exchange reaction. The probable loss of the last inner sphere water molecule from Tm to Yb illustrates the strong steric constraints imposed on the water binding site by the shrinking of the ionic radius of the center metal. The expectation that this would lead to a high water exchange rate is fully met by the measured value of $(3.1 \pm 0.2) \times 10^7$ s^{-1} for Gd−EGTA. Figure 7 shows a comparison of the crystal structures of $[Gd(DOTA)(H_2O)]^-$,[34] $[Er(EGTA)(H_2O)]^-$,[16] and $[Tb(TETA)]^-$,[35] which illustrates how the steric strain on the water binding site increases as the metal ion sinks deeper into the ligand cavity. In $[Gd(DOTA)(H_2O)]^-$ the water molecule occupies a capping position above the square plane formed by four oxygens of the acetate groups and presents an exchange rate of $(4.1 \pm 0.2) \times 10^6$ s^{-1}.[28] In $[Gd(EGTA)(H_2O)]^-$ the ethyl group bridging the two coordinating oxygens causes a steric compression of these atoms around the site occupied by the water molecule. This destabilizes the bound water molecule, resulting in an acceleration of the exchange rate by nearly 1 order of magnitude. In the last case, the conformational requirements of the macrocyclic ring cause the buckling of the nitrogen atoms which, in turn, affects the relationship of the oxygen atoms of the coordinating carboxylates. The resulting position of the acetate groups completely closes off the accessibility of the metal atom to the water molecule.

Simultaneous Treatment of EPR, ^{17}O NMR, and NMRD Data. The obtained dynamic parameters are compared with

(29) Koenig, S. H.; Brown, R. D. III. *Prog. Nucl. Magn. Reson. Spectrosc.* **1991**, *22*, 487.
(30) Bloembergen, N. *J. Chem. Phys.* **1957**, *27*, 572.
(31) Solomon, I. *Phys. Rev.* **1955**, *99*, 559.
(32) Freed, J. H. *J. Chem. Phys.* **1978**, *68*, 4034.
(33) Pubanz, D.; González, G.; Powell, D. H.; Merbach, A. E. *Inorg. Chem.* **1995**, *34*, 4447.
(34) (a) Dubost, J.-P.; Leger, M.; Langlois, M.-H.; Meyer, D.; Schaefer, M. *C. R. Acad. Sci., Ser. II* **1991**, *312*, 349. (b) Chang, C. A.; Francesconi, I. C.; Malley, M. F.; Kumar, K.; Gougoutas, J.Z.; Tweedle, M. F.; Lee, D. W.; Wilson, L. J. *Inorg. Chem.* **1993**, *32*, 3501.
(35) Spirlet, M.-R.; Rebizant, J.; Loncin, M.-F.; Desreux, J. F. *Inorg. Chem.* **1984**, *23*, 4278.

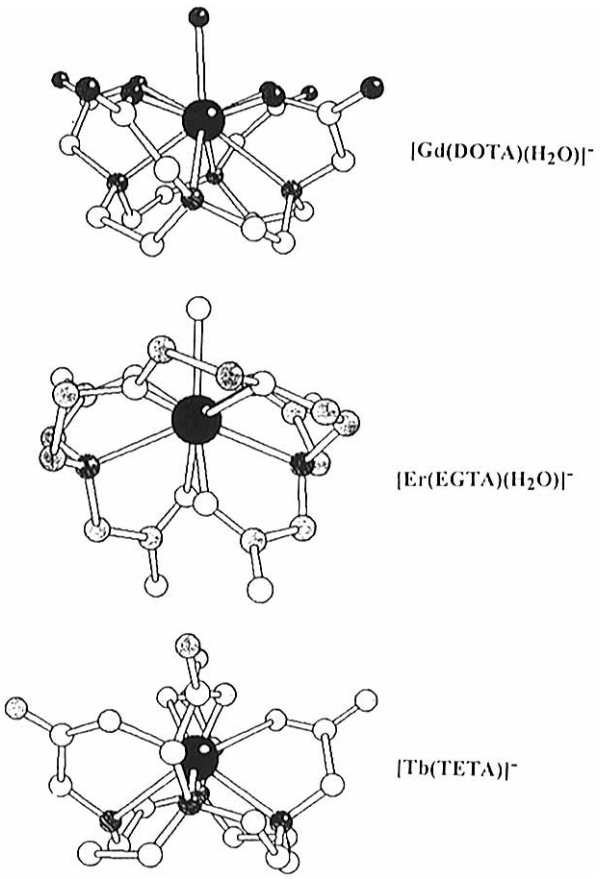

Figure 7. Comparison of the crystal structures of $[Gd(DOTA)(H_2O)]^-$, $[Er(EGTA)(H_2O)]^-$, and $[Tb(TETA)]^-$.

the corresponding values for several other Gd^{3+} complexes in Table 2.

Structural Parameters. The only parameters relevant to the structure of the complexes that are obtained from the combined fit are r_{GdO} and $A/\hbar$. The former is heavily influenced by the interplay with the quadrupolar coupling constant, and we do not attach any significance to the variation of these two parameters from one complex to another. The scalar coupling constant, $A/\hbar$, determined from the ^{17}O NMR shifts, is a measure of the Gd^{3+} spin density at the ^{17}O nucleus. The value should be approximately the same for all 9-coordinate, $q = 1$ complexes, since r_{GdO} does not vary significantly. The values for the different contrast agents are indeed very similar. This is evidence that our assumption of one inner sphere water molecule is correct, since the number of water molecules enters directly in our calculation of $\Delta\omega_r$, and is in agreement with our specific structural studies.

The lack of chemical shift data in the slow exchange region for $[Gd(EGTA)(H_2O)]^-$ forced us to fix the outer sphere constant C_{os}. A value of 0.1 was chosen, which seems reasonable in comparison with previous results[1,25,28] and yields a better fit of the shift data than values of either 0.0 or 0.2. The ^{17}O chemical shift data in the fast exchange region clearly shows a nonCurie behavior. We exclude experimental artifacts as well as coordination equilibria as the reason, but have not yet found a satisfactory explanation.

Electronic Relaxation. The theory governing electronic relaxation rates and their effect on NMR relaxation rates is undoubtedly the least well understood part of our data analysis. Electronic relaxation in Gd^{3+} complexes has generally been explained in terms of a zero field splitting interaction. Our previous ^{17}O NMR measurements have led us to propose that there is an additional spin-rotational contribution to the electronic relaxation rates.[25,28] Our high-field EPR measurements have demonstrated an intermolecular, diffusion-modulated dipole−dipole relaxation mechanism.[1] At the concentrations used for the NMR experiments, however, the intermolecular contribution to electronic relaxation is negligible. The main purpose of quantitative description of the concentration dependent contribution is to be able to use EPR line widths (especially at high fields) as an independent access to longitudinal electronic relaxation.

The $[Gd(EGTA)(H_2O)]^-$ complex has a slightly lower fitted Δ^2 value than other linear complexes. This difference may be an artifact from the inadequacy of the theory relating longitudinal electronic relaxation rates to proton relaxivity, and thus it should not be regarded as significant. The macrocyclic $[Gd(DOTA)(H_2O)]^-$ complex, however, has a significantly lower value of Δ^2. This suggests that the instantaneous structure of macrocyclic complexes is more symmetric than those of the linear complexes. The τ_v^{298} value is similar for all linear complexes, but much shorter for the macrocyclic complex; thus it can apparently change its distortion axes even more quickly than the other linear complexes.

The spin-rotation mechanism was invoked in order to explain the slower than expected decrease of $1/T_{1e}$ with magnetic field implied by the ^{17}O NMR relaxation data. The values obtained for the mean-square deviation of the **g**-tensor, δg_L^2, are quite reasonable compared to those found for Cu^{2+} complexes,[36] and there is no reason why a spin-rotation relaxation mechanism should not operate. In principle, the δg_L^2 values are a measure of the degree of permanent distortion of the complexes. However, we do not attach any significance to the variation of δg_L^2 from one complex to another as it is certainly affected by inadequacies in the description of the electronic relaxation rates due to the zero field splitting interaction.

Rotation. The absolute values of the rotational correlation times, τ_R^{298}, have to be treated with caution for the reasons explained in the first section of the discussion. For the low molecular weight compounds treated in this study they are not the prime concern. However, the τ_R^{298} values in Table 2 are reasonably well correlated with the size of the molecules, increasing from the aqua ion to the bulkier poly(amino carboxylate) complexes.

Water Exchange Kinetics. The picture of water exchange on lanthanide(III) complexes that we have built up over a series of publications[25,28,37−45] is intimately related to the coordination of the complexes in solution. The coordination number of the lanthanide(III) aqua ions is known to change from 9 for the early members of the series to 8 for the late members, as a result of the lanthanide contraction.[39,41,46,47] The members near the middle of the series (e.g., Sm^{3+}) exhibit a coordination

(36) Poupko, R.; Luz, Z. *J. Chem. Phys.* **1972**, *57*, 3311.
(37) Micskei, K.; Powell, D. H.; Helm, L.; Brücher, E.; Merbach A. E. *Magn. Reson. Chem.* **1993**, *31*, 1011.
(38) Cossy, C.; Barnes, A. C.; Enderby, J. E.; Merbach, A. E. *J. Chem. Phys.* **1988**, *90*, 3254.
(39) Cossy, C.; Powell, D. H.; Helm, L.; Merbach, A. E. *New J. Chem.* **1995**, *19*, 27.
(40) Powell, D. H.; Favre, M.; Graeppi, N.; Ni Dhubhghaill O. M.; Pubanz, D.; Merbach, A. E *J. Alloys Compd.* **1995**, *225*, 246.
(41) Kowall, T.; Foglia, F.; Merbach A. E. *J. Am. Chem. Soc.* **1995**, *117*, 3790.
(42) Kowall, T.; Foglia, F.; Helm, L.; Merbach A. E. *Chem. Eur. J.* **1996**, *2*, 285.
(43) Cossy, C.; Helm, L.; Merbach, A. E. *Inorg. Chem.* **1988**, *27*, 1973.
(44) Powell, D. H.; Merbach, A. E. *Magn. Reson. Chem.* **1994**, *32*, 739.
(45) Tóth, É.; Pubanz, D.; Vauthey, S.; Helm, L.; Merbach, A. E. *Chem. Eur. J.* **1996**, *2*, 1607.
(46) Spedding, F. H.; Pikal, R. J.; Ayres, B. O. *J. Phys. Chem.* **1966**, *70*, 2440.
(47) Swaddle, T. W. *J. Inorg. Bioinorg. Mech.* **1983**, *2*, 98.

equilibrium between the octaaqua and enneaaqua complexes.[39] The exchange rates for the late, 8-coordinate lanthanide aqua ions from Yb^{3+} to Gd^{3+} increase toward the middle of the lanthanide series,[43] while the negative activation volumes indicate an associatively activated exchange mechanism.[39] The increase in exchange rates for all of these octaaqua ions toward the center of the lanthanide series is interpreted as being due to the relative stabilization of the 9-coordinate transition state as the size of the lanthanide(III) ion increases.

For the 8-coordinate poly(amino carboxylate) complex $[Gd(PDTA)(H_2O)]^-$, the exchange rate is smaller by almost 1 order of magnitude and the activation volume is less negative. This indicates that its coordination sphere is considerably more crowded, slowing down the rate-determining entrance of the incoming water molecule into the first coordination sphere.

The remaining poly(amino carboxylate) complexes in Table 2 are, on the other hand, 9-coordinate Gd^{3+} complexes. Their positive activation volumes demonstrate that the water exchange mechanism is dissociatively activated, i.e., the transition state in the exchange process resembles an 8-coordinate species. It was shown previously that the 8-coordinate transition state can be stabilized with respect to the 9-coordinate ground state to speed up the water exchange rate by reducing the ionic radius of the center metal, which raises the steric constraint of the water binding site.[33] An analogous effect can be reached by certain changes in the ligand structure, as is discussed in the next section.

On changing from $[Gd(DTPA\text{-}BMA)(H_2O)]$ to $[Gd(DTPA)(H_2O)]^{2-}$ two amide ligating groups are replaced by more strongly ligating carboxylate groups. These more strongly coordinating groups can be expected to pull the ligand more tightly around the metal center, thus increasing the crowding at the water binding site. This favors the dissociative exchange mechanism (indicated by the large positive activation volume) giving the observed increase of water exchange rate (Table 2). The same reflection holds true for $[Gd(EGTA)(H_2O)]^-$, though there are only four carboxylate groups instead of five, and two theoretically only loosely coordinating oxygen atoms of the ether groups. The latter, however, belong to the backbone of the multidentate ligand and thus are pulled tightly into the first coordination sphere, resulting in high steric constraints on the water binding site (see also Figure 7). This view is corroborated by the results of our structural study, which indicates that for the last members of the lanthanide series the inner sphere water is lost due to the steric constraint on its binding site. From this and the high value of the exchange rate one should expect that of all of the CN = 9 and $q = 1$ gadolinium(III) poly(amino carboxylate) complexes hitherto investigated the $EGTA^{4-}$ complex has the smallest free energy difference between the 9- and 8-coordinated states and, thus, should also display a largely positive activation volume. The value of $+10.5 \pm 1.0$ cm^3 mol^{-1} suggests indeed a limiting dissociative *D* mechanism.

Implications for Maximizing Relaxivity. In order to improve on the relaxivity of the Gd complexes currently used as contrast agents for MRI, one has to shorten τ_M and to maximize τ_R and T_{1e}. Research has hitherto concentrated successfully on τ_R by linking the complex to a macromolecular substrate, either covalently or not. We now have the tools to tune τ_M and may speculate on the effect of T_{1e}. Several important observations can be made: if the contrast agent is fixed to a polymer that is prone to anisotropic motion, as are for example dendritic macromolecules,[45] much of the potential benefit gets lost; one has to achieve rigid linking to a polymer with as low a segmental motion as possible. A really big boost, however, can only be attained if one succeeds not only in freezing out rotation and accelerating water exchange to the proper amount but also in slowing down electronic relaxation.

Acknowledgment. The Lausanne group thanks Dr. L. Helm for useful discussions, Dr. U. Frey for his help with the high-pressure NMR equipment, and Nycomed Inc. for financial support. Their work has been financially supported by the Swiss National Science Foundation (Grant No. 45419.95) and the Swiss OFES as part of the European COST D1 Action. We thank Nicole Graeppi for measuring the UV spectra of the Ce and Eu complexes. The Torino group is indebted to Bracco S.p.A. (Milano, Italy) and to Italian CNR (Progetto Strategico Tecnologie Chimiche Innovative) for financial support and to EU-Large Scale Facility at the University of Florence, Italy, for the use of the FC-relaxometer.

Supporting Information Available: Text giving full details of the simultaneous fitting of EPR, NMRD, and ^{17}O NMR data, listings of reduced transverse and longitudinal ^{17}O relaxation rates and reduced angular frequencies of aqueous solutions containing $[Gd(EGTA)(H_2O)]^-$ at 1.4 (Table S1a), 4.7 (Table S1b), 9.4 (Table S1c), and 14.1 T (Table S1d) and transverse electronic relaxation rates of $[Gd(EGTA)(H_2O)]^-$ at the X-band and the 2-mm band (Table S1e) as a function of temperature, proton relaxivities of $[Gd(EGTA)(H_2O)]^-$ in saline buffer at 278.2 (Table S1f), 286.2 (Table S1g), 298.2 (Table S1h), and 307.2 K (Table S1i) as a function of magnetic field (expressed as proton resonance frequency), chemical shifts and values of $\delta/\langle S_Z\rangle$ and $C_D/\langle S_Z\rangle$ of the Ac1 and Ac1′ protons at 298 K (Table S2), variable temperature ^1H NMR spectra (400 MHz, La (Figure S1a), Eu (Figure S1f), Lu (Figure S1o); 90 MHz, Ce (Figure S1b), Pr (Figure S1c), Nd (Figure S1d), Sm (Figure S1e), Tb (Figure S1g), Dy (Figure S1h), Ho (Figure S1i), Er (Figure S1l), Tm (Figure S1m), Yb (Figure S1n)) and ^{13}C NMR spectra (100.6 MHz, La (Figure S2a), Eu (Figure S2f), Lu (Figure S2o); 22.4 MHz, Ce (Figure S2b), Pr (Figure S2c), Nd (Figure S2d), Sm (Figure S2e), Tb (Figure S2g), Dy (Figure S2h), Ho (Figure S2i), Er (Figure S2l), Tm (Figure S2m), Yb (Figure S2m)) at 298 K for all of the $[Ln(EGTA)(H_2O)]^-$ complexes with the exception of Pm and Gd, variable temperature ^{13}C NMR spectra of $[Eu(EGTA)(H_2O)]^-$ at 2.1 T (Figure S3), proton relaxivities R_1 ($mmol^{-1}$ s^{-1} kg) of $[Gd(EGTA)(H_2O)]^-$ and $[Gd(DTPA)(H_2O)]^{2-}$ in aqueous solution at 20 MHz and variable temperature (Figure S4), and UV spectra of $[Ce(EGTA)(H_2O)_x]^-$ as a function of temperature and pressure (Figure S5) and thermodynamic data calculated from these spectra (Table S3) (38 pages). Ordering information is given on any current masthead page.

IC970240O